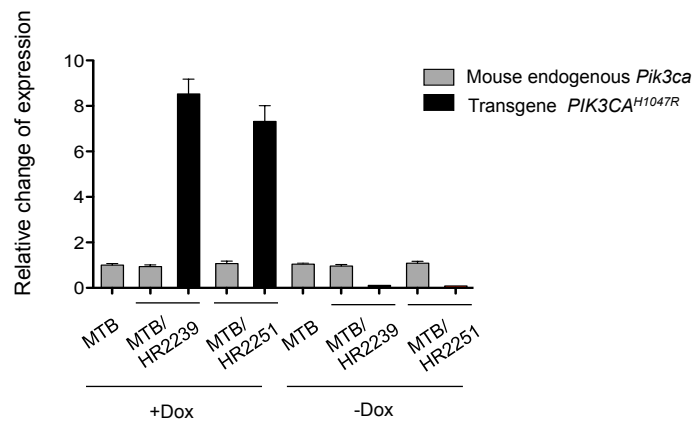
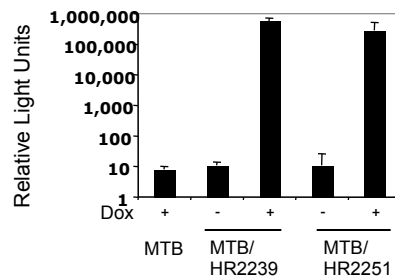
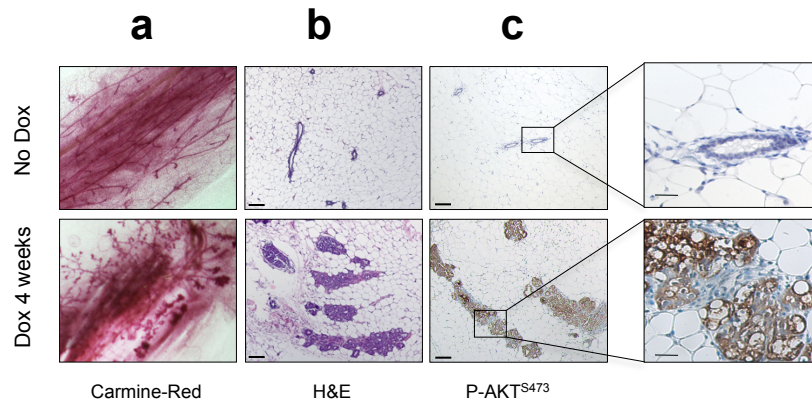


Supplementary Information Titles

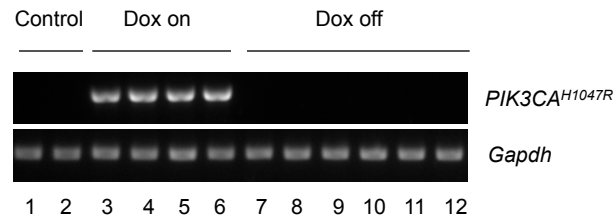
Journal: Nature Medicine	
Article Title:	Oncogenic <i>PIK3CA</i> -driven mammary tumors frequently recur via PI3K pathway-dependent and -independent mechanisms
Corresponding Author:	Jean J. Zhao (jean_zhao@dfci.harvard.edu)
Supplementary Item & Number	Title or Caption
Supplementary Fig.1 Fig.2 Fig.3 Fig.4 Fig.5 Fig.6 Fig.7 Fig.8 Fig.9 Fig.10 Fig.11 Fig.12 Fig.13 Fig.14 Fig.15 Fig.16	<p>Doxycycline-inducible expression of <i>PIK3CA</i>^{H1047R}</p> <p>Analyses of early mammary cancer lesions</p> <p>The expression of <i>PIK3CA</i>^{H1047R} is suppressed following doxycycline withdrawal</p> <p>Tumor responses to doxycycline withdrawal</p> <p>Mouse SNP6.0 array analyses of mammary tumors</p> <p>Amplification of <i>c-Myc</i> in RCT-D419 and RCT-C658 tumors</p> <p>A fraction of recurrent tumors have increased <i>c-Myc</i> copy number</p> <p>A fraction of recurrent tumors have increased <i>c-Myc</i> mRNA expression</p> <p>A fraction of recurrent tumors have increased <i>c-Myc</i> protein</p> <p>Frequencies of <i>c-Myc</i> up-regulation in recurrent tumors</p> <p>A fraction of recurrent tumors have increased <i>c-Met</i> mRNA expression</p> <p>A fraction of recurrent tumors have increased <i>Mdm2</i> mRNA expression</p> <p>Increased <i>c-Met</i> expression in the RCT-E565 tumor</p> <p>Increased <i>c-Myc</i> expression in RCT-D419 and RCT-C658 tumors</p> <p>Overexpression of <i>c-Myc</i> renders tumors resistance to GDC-0941</p> <p>Co-occurrence of <i>PIK3CA</i> mutation with <i>c-MYC</i> elevation in human breast tumors</p>
Supplementary Table 1 Table 2 Table 3	<p>A summary of primary tumors' histopathological phenotypes and their respective response following inactivation of <i>PIK3CA</i>^{H1047R}</p> <p>A summary for recurrent tumors scored with increased expression levels of <i>c-Myc</i>, <i>c-Met</i> and <i>Mdm2</i></p> <p>Reverse-Phase Protein Array (RPPA) analysis of <i>c-MYC</i> protein levels for a cohort of breast tumor samples with annotated <i>PIK3CA</i> mutation status</p>
Supplementary Methods	Supplementary Methods

a**b**

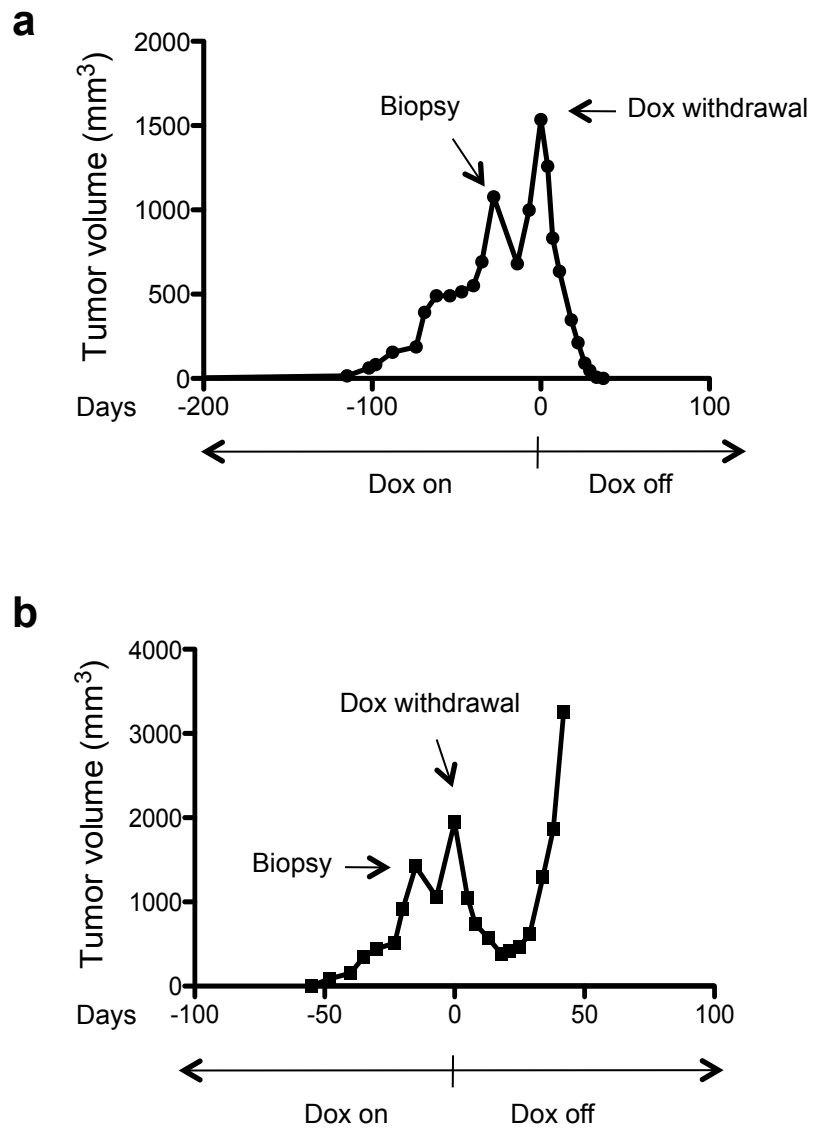
Supplementary Fig. 1 Doxycycline-inducible expression of *PIK3CA^{H1047R}*. (a) Quantitative reverse transcription polymerase chain reaction (qRT-PCR) analysis of *PIK3CA^{H1047R}* Transgene expression and endogenous *Pik3ca* expression in mammary tissues isolated from MTB/HR-2239 and MTB/HR-2251 mice in the presence (+) or absence (-) of doxycycline. Mouse *Gapdh* was used as an endogenous control. The expression levels of transgene *PIK3CA^{H1047R}* and endogenous *Pik3ca* in both bi-transgenic mouse lines were calculated relative to the endogenous *Pik3ca* expression in control mice (MTB). (b) Luciferase activity in mammary tissues isolated from MTB/HR-2239 and MTB/HR-2251 mice in the presence (+) or absence (-) of doxycycline.



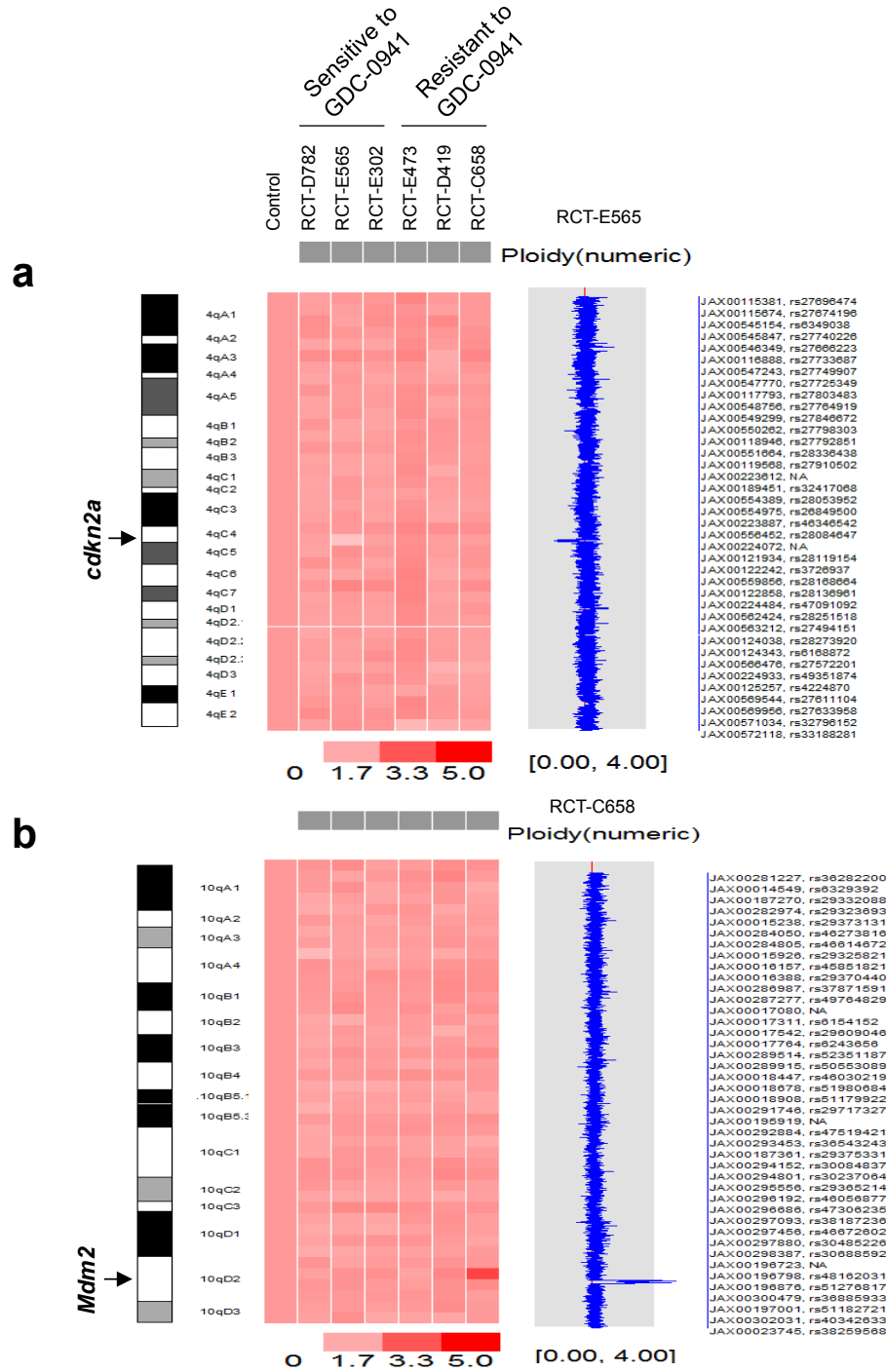
Supplementary Fig. 2 Analyses of early mammary cancer lesions. A cohort of 8-week old $iPIK3CA^{H1047R}$ females ($n=5$) were treated with doxycycline for 4 weeks, and their mammary glands were harvested for analysis. Carmine-stained whole mounts (**a**), hematoxylin and eosin (H&E)-stained (**b**), and anti-phospho-AKT (Ser473) IHC sections (**c**) of mammary glands from $iPIK3CA^{H1047R}$ female mice induced with doxycycline for 4 weeks (lower panels) or uninduced (No Dox, upper panels) as control. Scale bars, $100\mu\text{m}$. The insets are shown magnified, scale bars, $25\mu\text{m}$.



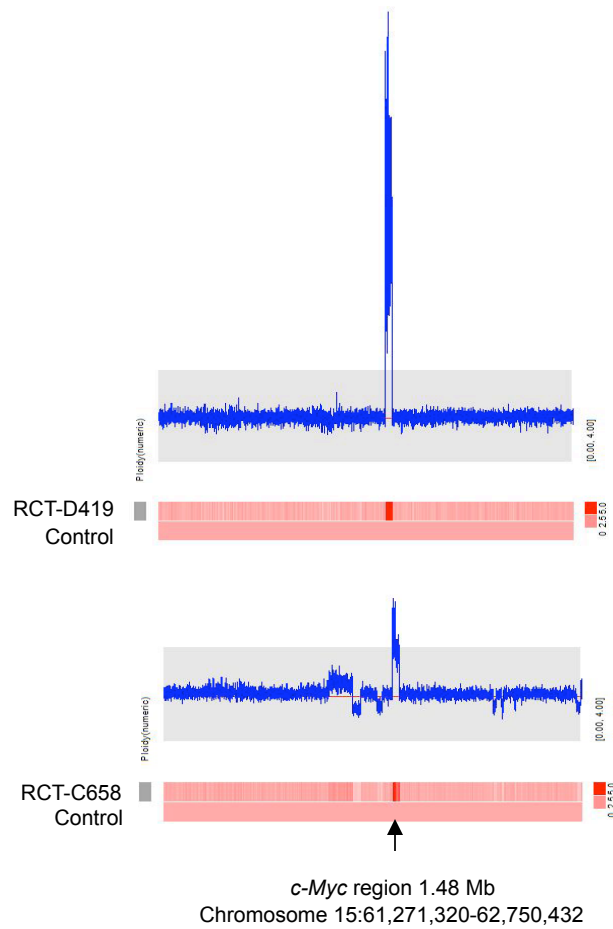
Supplementary Fig. 3 The expression of *PIK3CA^{H1047R}* is suppressed following doxycycline withdrawal. RNA samples were isolated from mammary tumors from mice maintained on doxycycline (lanes 3-6) or 6 days following doxycycline withdrawal (lanes 7-12). Samples isolated from mammary tissues of mice that had not been induced by doxycycline were used as controls (lanes 1 and 2). The levels of the *PIK3CA^{H1047R}* transgene mRNA were determined by RT-PCR. *Gapdh* was used as a control.



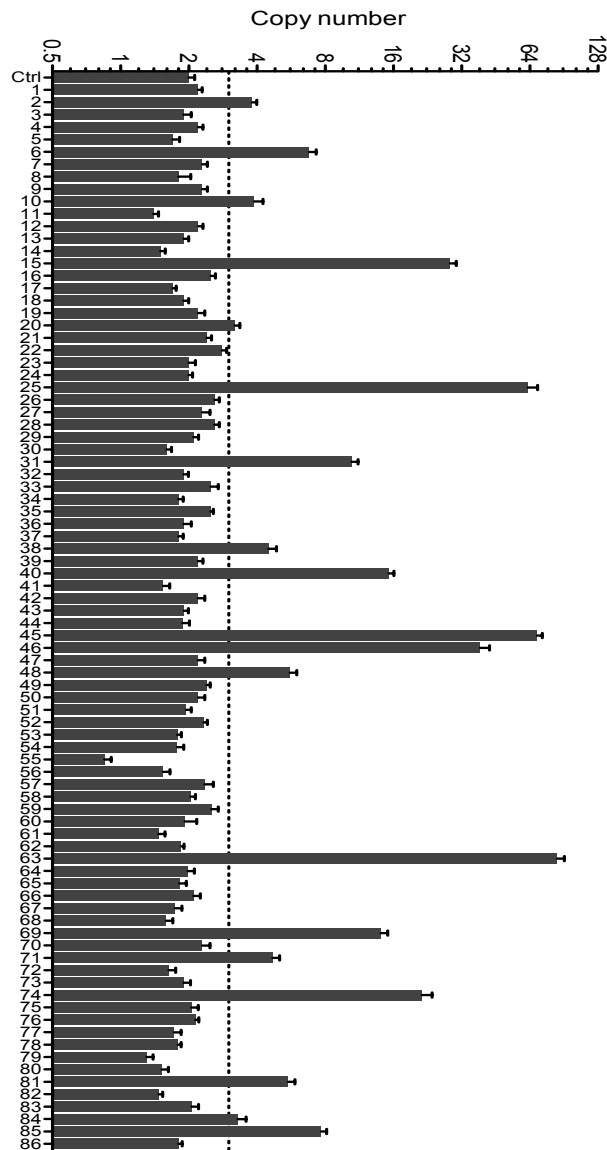
Supplementary Fig. 4 Tumor responses to doxycycline withdrawal. Representative graphs showing tumor growth on doxycycline and regression to a completely tumor-free state following doxycycline withdrawal (**a**), or partial regression followed by subsequent re-growth in the absence of doxycycline (**b**).



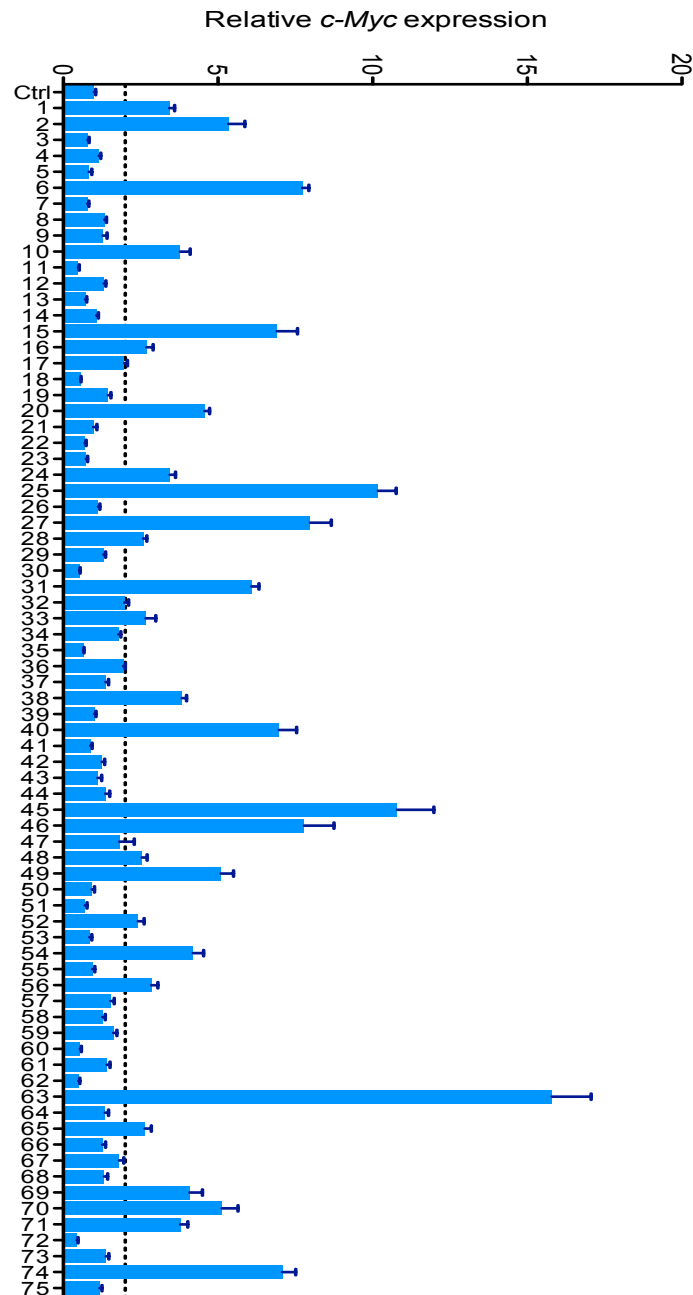
Supplementary Fig. 5 Mouse SNP6.0 array analyses of mammary tumors. Mouse SNP6.0 array analyses of six *PIK3CA*^{H1047R}-independent recurrent tumors identified a single copy loss in the *Cdkn2a* locus in RCT-E565 (a) and a focal amplification encompassing the *Mdm2* locus in RCT-C658 (b).



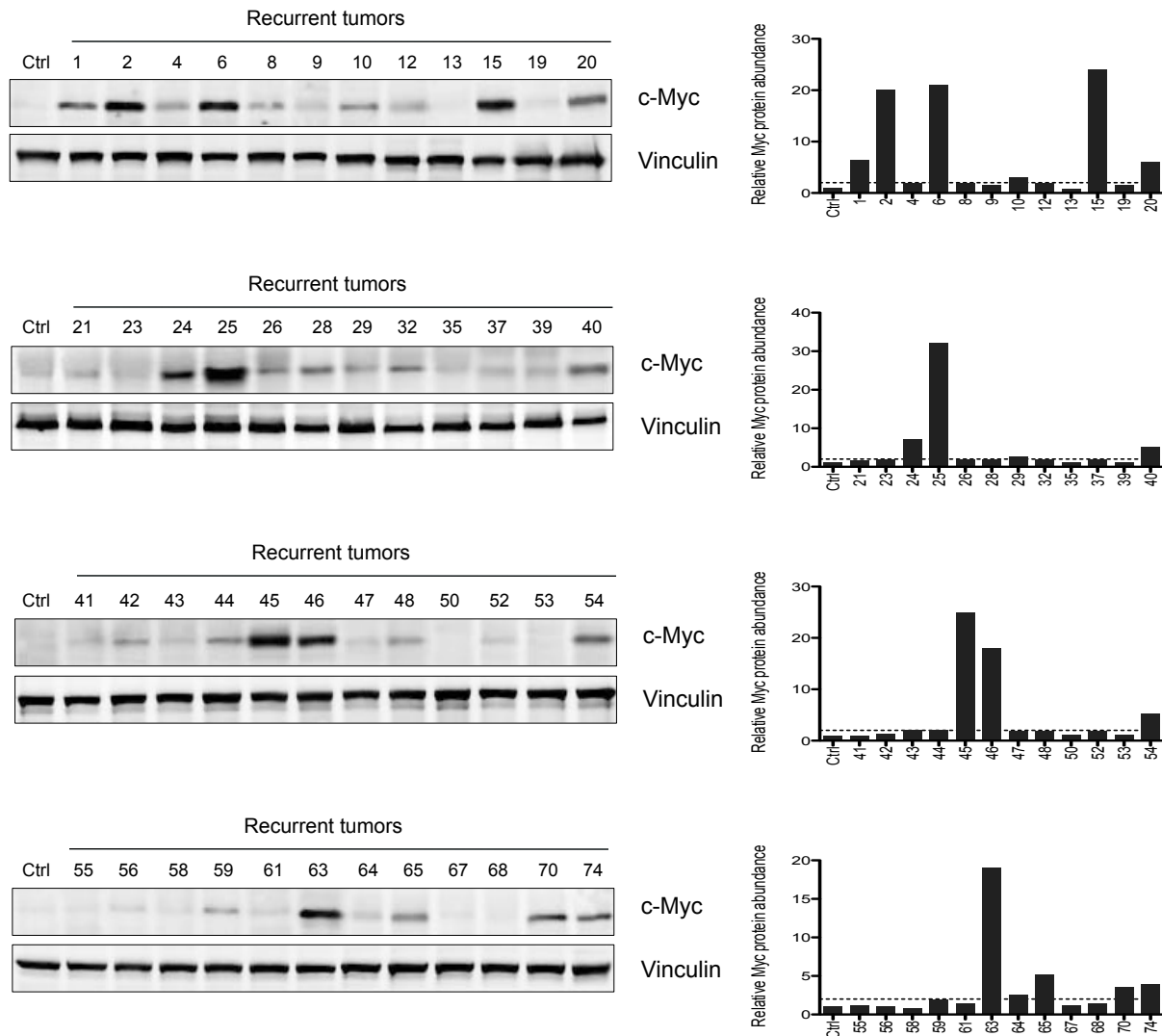
Supplementary Fig. 6 Amplification of *c-Myc* in RCT-D419 and RCT-C658 tumors. Mouse SNP6.0 array analyses of *PIK3CA^{H1047R}*-independent recurrent tumors, RCT-D419 and RCT-C658, demonstrating common focal amplification at the *c-Myc* locus.



Supplementary Fig. 7 A fraction of recurrent tumors have increased *c-Myc* copy number. Copy numbers of *c-Myc* were analyzed using quantitative PCR (qPCR) with genomic DNAs isolated from all 86 recurrent tumors collected. Genomic DNAs isolated from mammary gland tissues of iPIK3CA^{H1047R} mice that had not been treated with doxycycline were used as a control (copy number =2). The dotted line indicates three copies. Results are shown as mean \pm SD of triplicate experiments. Mouse *Tfrc* was used as a reference control.



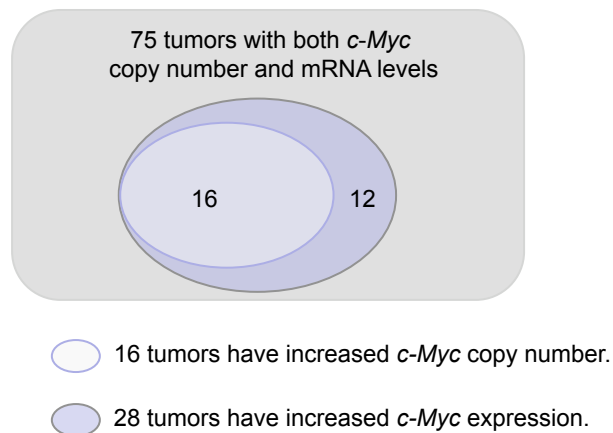
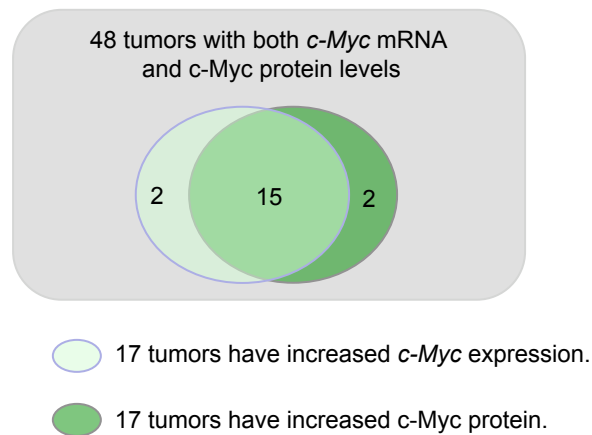
Supplementary Fig. 8 A fraction of recurrent tumors have increased *c-Myc* mRNA expression. Expression levels of *c-Myc* in 75 of 86 recurrent tumors that yielded good quality RNAs were analyzed by qRT-PCR. RNAs isolated from mammary gland tissues in iPIK3CA^{H1047R} mice that had not been treated with doxycycline were used as a control. The dotted line indicates the relative mRNA value at 2. Results are shown as mean \pm SD of triplicate experiments.



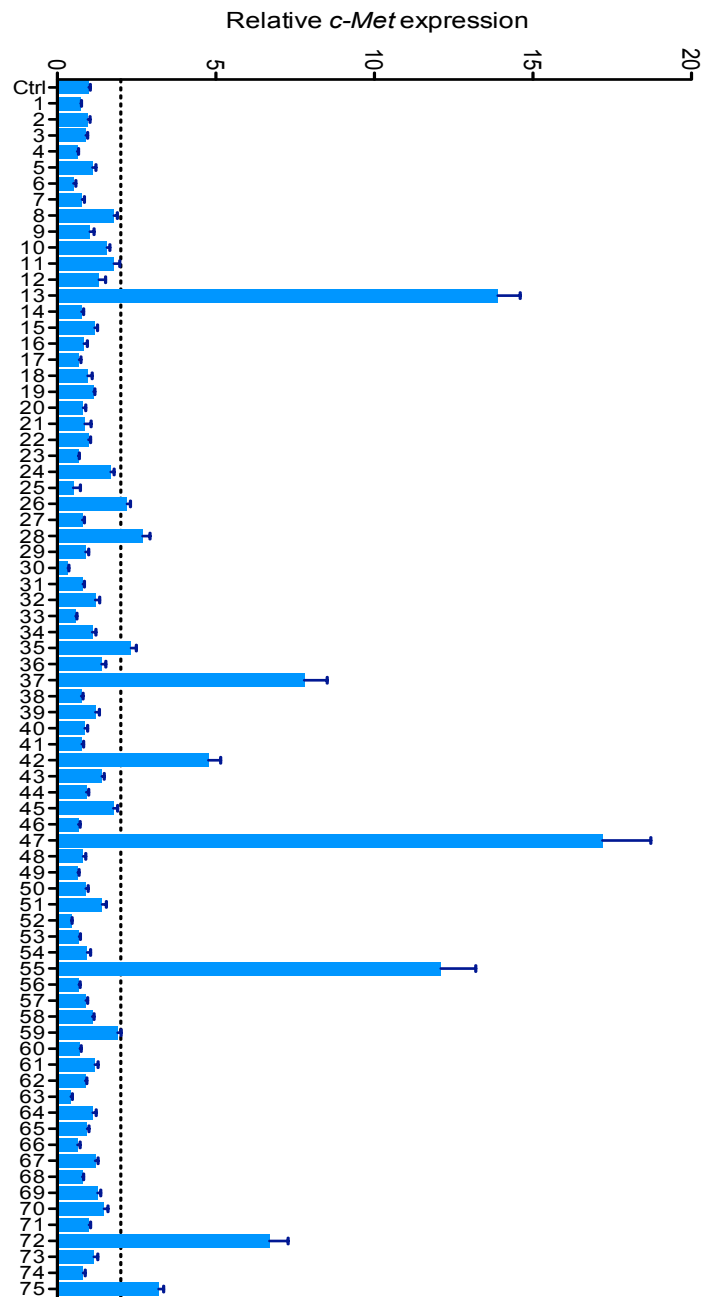
Supplementary Fig. 9 A fraction of recurrent tumors have increased c-Myc protein. Protein levels of c-Myc in 48 out of 86 recurrent tumors that yielded sufficient tumor lysates were analyzed by Western blot analysis. Cell lysates isolated from mammary tissues of *iPIK3CA^{H1047R}* mice that had not been treated with doxycycline were used as controls. Vinculin was used as a loading control. Bar graphs reflect mean values of relative c-Myc protein levels in recurrent tumors from two experiments. The dotted lines indicate a baseline of relative c-Myc protein level at 2.

a

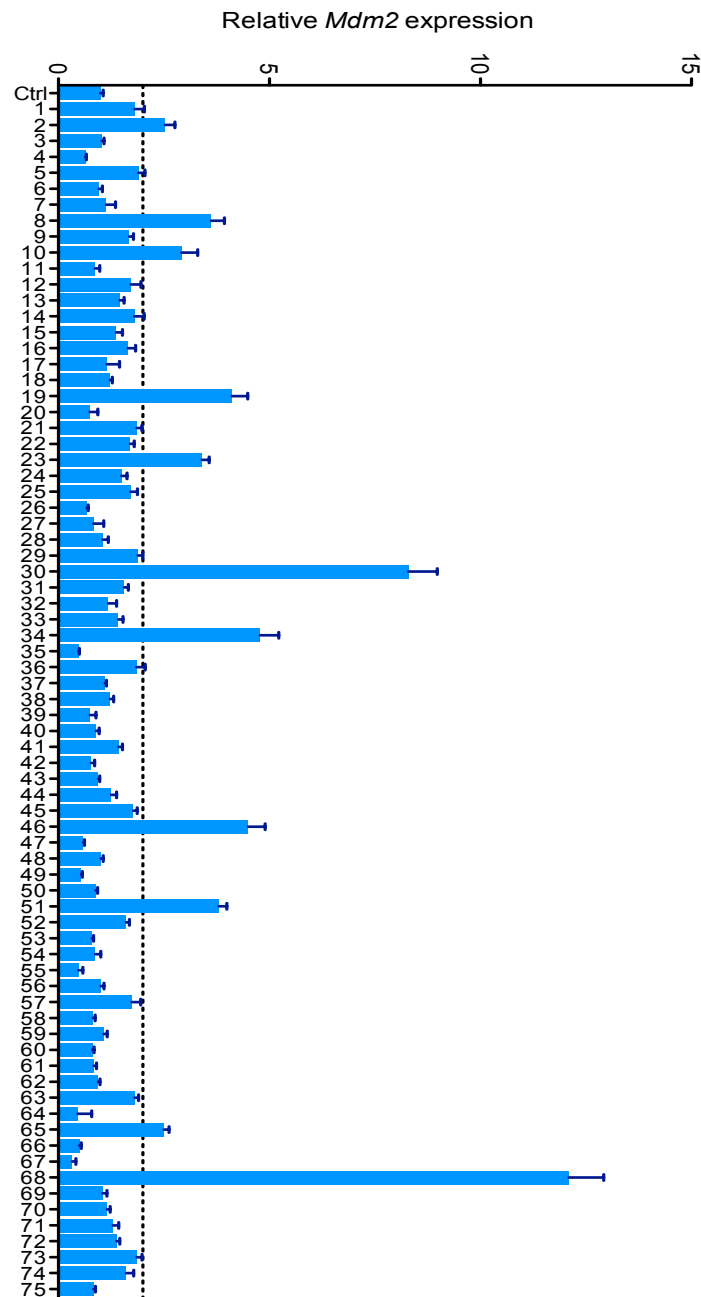
c-Myc status in recurrent tumors	Frequency
Increased copy number	19/86 (22%)
Increased mRNA expression	28/75 (37%)
Increased protein abundance	17/48 (35%)

b**c**

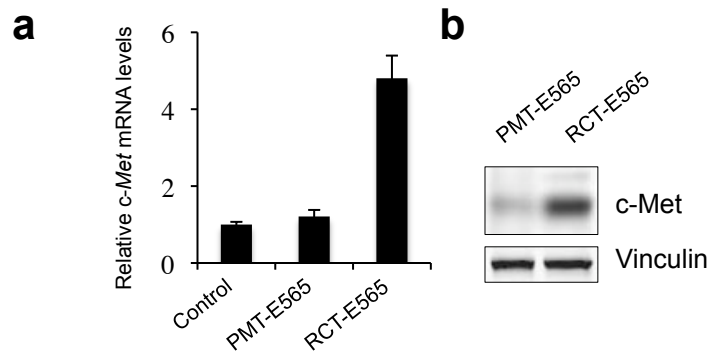
Supplementary Fig. 10 Frequencies of c-Myc up-regulation in recurrent tumors. (a) Frequencies of increased *c-Myc* at copy number, mRNA expression and protein levels in recurrent tumors are summarized. (b) All the tumors with increased *c-Myc* copy number also have increased *c-Myc* mRNA expression. The frequency of increased *c-Myc* mRNA expression (28/75, 36%) in recurrent tumors is higher than that of *c-Myc* amplification (16/75, 21%) ($P = 0.048$, Fisher's exact test). (c) Of the 48 tumors examined by western blot analysis, 17 have increased *c-Myc* protein levels and 15 of these are correlated with increased *c-Myc* mRNA expression levels.



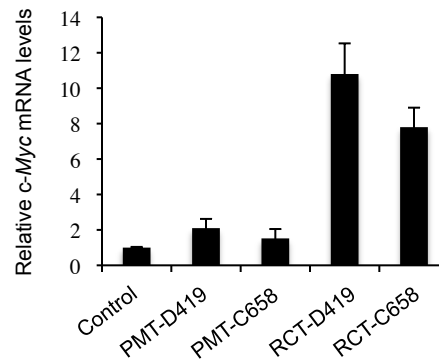
Supplementary Fig. 11 A fraction of recurrent tumors have increased *c-Met* mRNA expression. Expression levels of *c-Met* in 75 of 86 recurrent tumors that yielded good quality RNAs were analyzed by qRT-PCR. RNAs isolated from mammary gland tissues in iPIK3CA^{H1047R} mice that had not been treated with doxycycline were used as a control. The dotted line indicates the relative mRNA value at 2. Results are shown as mean \pm SD of triplicate experiments.



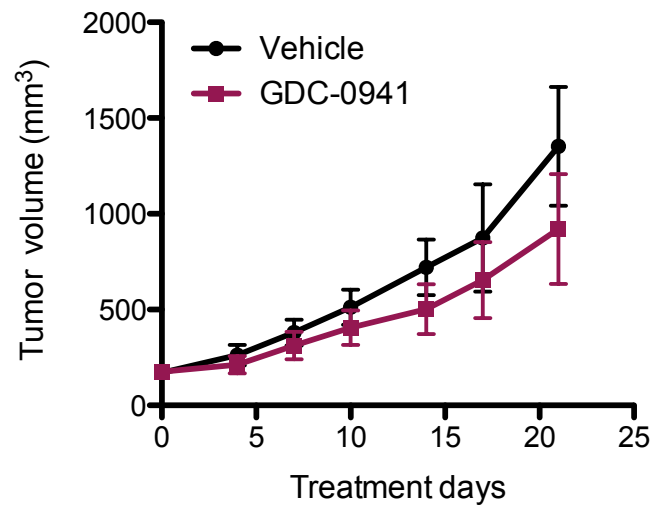
Supplementary Fig. 12 A fraction of recurrent tumors have increased *Mdm2* mRNA expression. Expression levels of *Mdm2* in 75 of 86 recurrent tumors that yielded good quality RNAs were analyzed by qRT-PCR. RNAs isolated from mammary gland tissues in iPIK3CA^{H1047R} mice that had not been treated with doxycycline were used as a control. The dotted line indicates the relative mRNA value at 2. Results are shown as mean \pm SD of triplicate experiments.



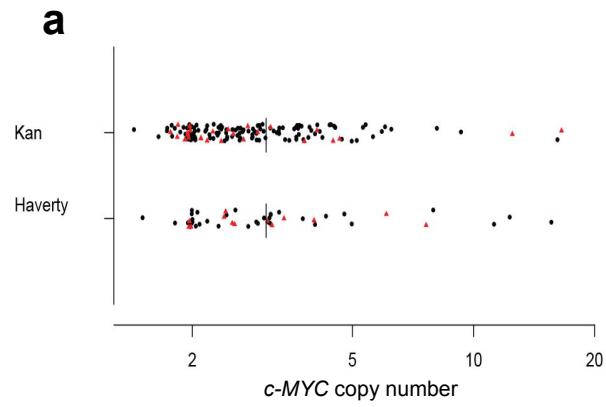
Supplementary Fig. 13 Increased c-Met expression in the RCT-E565 tumor. **(a)** qRT-PCR analysis of *c-Met* expression in RCT-E565 and its respective tumor biopsy obtained before doxycycline withdrawal (PMT-E565). **(b)** Western blot analysis of c-Met levels in PMT-E565 and RCT-E565 tumor samples. Vinculin was used as a loading control.



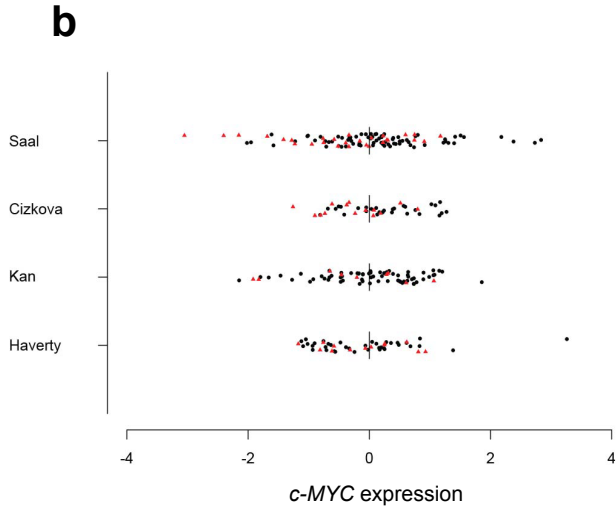
Supplementary Fig. 14 Increased *c-Myc* expression in RCT-D419 and RCT-C658 tumors. qRT-PCR analysis of *c-Myc* expression in RCT-D419 and RCT-C658 and their respective tumor biopsies, PMT-D419 and PMT-C658, obtained before doxycycline withdrawal as indicated. Uninduced normal mammary tissues were used as a control. Results are shown as mean \pm SD of triplicate experiments.



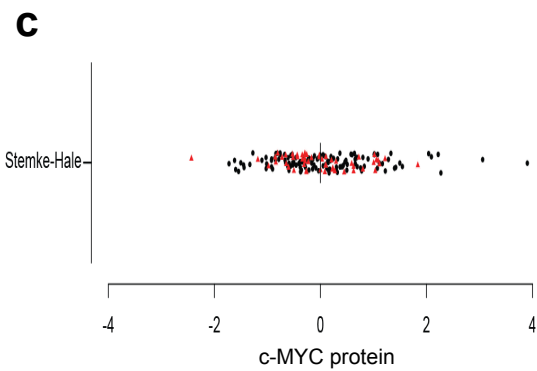
Supplementary Fig. 15 Overexpression of c-Myc renders tumors resistance to GDC-0941. Mice bearing D777-Myc(WT) tumors were treated with either GDC-0941 (120 mg/kg/day) or vehicle and tumor growth followed. Data are shown as mean \pm S.E.M ($n = 6$).



Breast cancer dataset	Number of tumors	Proportion <i>PIK3CA</i> mut	Proportion of <i>PIK3CA</i> mut tumors with <i>MYC</i> copy number > 3
Kan et al	145	26/145 (18%)	7/26 (27%)
Haverty et al	51	13/51 (26%)	6/13 (46%)



Breast cancer dataset	Number of tumors	Proportion <i>PIK3CA</i> mut	Proportion of <i>PIK3CA</i> mut tumors with <i>MYC</i> expression > mean level
Saal et al	104	28/104 (27%)	10/28 (36%)
Cizkova et al	44	15/44 (34%)	5/15 (33%)
Kan et al	76	9/76 (12%)	4/9 (44%)
Haverty et al	51	13/51 (26%)	6/13 (46%)



Breast cancer dataset	Number of tumors	Proportion <i>PIK3CA</i> mut	Proportion of <i>PIK3CA</i> mut tumors with <i>MYC</i> protein > mean level
Stemke-Hale et al	179	53/179 (30%)	25/53 (47%)

Supplementary Fig. 16 Co-occurrence of PIK3CA mutation with c-MYC elevation in human breast tumors. (a) Distribution and summary table of copy numbers at the *c-MYC* locus in *PIK3CA* mutant and *PIK3CA* wild-type breast tumors in two independent cohorts for which these data are available. The black lines indicate three copies. (b) Distribution and summary table of *c-MYC* expression levels for *PIK3CA* mutant and wild type tumors (presented as in panel a) in four independent cohorts of breast tumors for which these data are available. The black lines indicate the mean value for each cohort, which was normalized to zero. Outliers with *c-MYC* gene expression $> \pm 4SD$ from mean were excluded from the plot. (c) Distribution and summary table of c-MYC protein expression in *PIK3CA* mutant and wild-type breast tumors (presented as in panel a) in a cohort for which these data are available. c-MYC protein levels were determined by RPPA (reverse phase protein array). The black lines indicate the mean value for each cohort, which was normalized to zero. *PIK3CA* mutant, red triangles; *PIK3CA* wild-type, black dots.

Pathology	Response following inactivation of <i>PIK3CA</i> ^{H1047R}		
	Fully regressed	Recurred	Subtotal
Solid*	30% (8/27)	70% (19/27)	33% (27/83)
Acinar	71% (5/7)	29% (2/7)	8% (7/83)
Glandular	25% (1/4)	75% (3/4)	5% (4/83)
Papillary	50% (5/10)	50% (5/10)	12% (10/83)
Squamous metaplasia	42% (5/12)	58% (7/12)	15% (12/83)
Mixed	43% (10/23)	57% (13/23)	28% (23/83)
Total	39% (32/83)	61% (51/83)	100% (83/83)

Supplementary Table 1. A summary of primary tumors' histopathological phenotypes and their respective response following inactivation of *PIK3CA*^{H1047R}. "Solid" tumors seem to be more likely to develop resistance following inhibition of the oncogenic *PIK3CA* (regressed tumors vs. recurrent tumors were analyzed by Fisher's exact test, **P* = 0.006). While 71% (5/7) "acinar" tumors fully regressed and 75% (3/4) "glandular" tumors recurred, the correlation between the tumor histology and response to the inactivation of *PIK3CA*^{H1047R} cannot be established with sufficient statistical power due to the small sample sizes. There was no correlation found in tumors displaying other pathological phenotypes with their response to *PIK3CA*^{H1047R} inactivation.

Tumor ID	<i>c-Myc</i>	<i>c-Met</i>	<i>Mdm2</i>
1	+		
2	+		+
3			
4			
5			
6	+		
7			
8			+
9			
10	+		+
11			
12			
13		+	
14			
15	+		
16	+		
17			
18			
19			+
20	+		
21			
22			
23			+
24	+		
25	+		
26		+	
27	+		
28	+	+	
29			
30			+
31	+		
32			
33	+		
34			+
35		+	
36			
37		+	
38	+		
39			
40	+		
41			
42		+	
43			
44			
45	+		
46	+		+
47		+	
48	+		
49	+		
50			
51			+
52	+		
53			
54	+		
55		+	
56	+		
57			
58			
59			
60			
61			
62			
63	+		
64			
65	+		+
66			
67			
68			+
69	+		
70	+		
71	+		
72		+	
73			
74	+		
75		+	
Frequency	37% (28/75)	13% (10/75)	15%(11/75)

Supplementary Table 2. A summary for recurrent tumors scored with increased expression levels of *c-Myc*, *c-Met* and *Mdm2*. Positive (+) represents a tumor sample having a relative expression level for *c-Myc*, *c-Met* or *Mdm2* two fold higher than normal controls as shown in Supplementary Figures 8, 11 and 12, respectively. Increased expression of *c-Myc* is seen in 28 of 75 (37%) recurrent tumors, which is significantly more frequent than increased expression levels of *c-Met* (13%, $P = 0.0012$, Fisher's exact test), and *Mdm2* (15%, $P = 0.0026$, Fisher's exact test).

Patient ID	PIK3CA Mutation status	c-MYC.txt		Patient ID	PIK3CA Mutation status	c-MYC.txt		Patient ID	PIK3CA Mutation status	c-MYC.txt
2976	PIK3CA E418K	-3.420004828		3067	WT	-4.157231292		1388	WT	-3.497497193
4877	PIK3CA E545K	-3.876099221		3044	WT	-4.108894749		1188	WT	-3.496686888
3969	PIK3CA E545K	-3.809618933		2043	WT	-4.083818388		2956	WT	-3.485117591
2917	PIK3CA E545K	-3.747966038		1576	WT	-4.008039293		4561	WT	-3.477370405
3552	PIK3CA E545K	-3.741051472		1229	WT	-3.973876172		4082	WT	-3.476280592
1253	PIK3CA E545K	-3.670196556		7333	WT	-3.972801477		3287	WT	-3.465608694
1202	PIK3CA E545K	-3.651609314		7222	WT	-3.968847901		1172	WT	-3.458410879
4226	PIK3CA E545K	-3.476285902		1385	WT	-3.928124991		2833	WT	-3.454156349
665	PIK3CA E545K	-3.426982732		230	WT	-3.92756436		663	WT	-3.451957867
3871	PIK3CA E545K	-3.320903612		3818	WT	-3.926773254		6995	WT	-3.447077745
1359	PIK3CA E545K	-3.165086945		3247	WT	-3.919089133		432	WT	-3.441108565
1580	PIK3CA E545K	-3.074691352		2127	WT	-3.898288809		4077	WT	-3.434535192
4255	PIK3CA E545K	-3.068736297		3354	WT	-3.89479672		7685	WT	-3.431155958
953	PIK3CA E545K	-3.037556221		1382	WT	-3.891890991		201	WT	-3.409626538
702	PIK3CA E545K	-3.02608429		3819	WT	-3.879407725		5328	WT	-3.386984026
4276	PIK3CA E545K/PIK3CA E418K	-3.258526787		4936	WT	-3.867360384		3122	WT	-3.386012791
3102	PIK3CA H1047R	-4.597086988		2966	WT	-3.857368736		1025	WT	-3.378254469
1386	PIK3CA H1047R	-4.042197155		7178	WT	-3.856087152		4197	WT	-3.37567469
4360	PIK3CA H1047R	-3.952784031		3926	WT	-3.818686141		7029	WT	-3.356948816
3973	PIK3CA H1047R	-3.896780459		70	WT	-3.814808445		3049	WT	-3.356142712
1450	PIK3CA H1047R	-3.891938914		1556	WT	-3.810481267		138	WT	-3.346374174
2177	PIK3CA H1047R	-3.839816517		1575	WT	-3.791809468		1328	WT	-3.335629506
1179	PIK3CA H1047R	-3.805187045		4013	WT	-3.789339344		3379	WT	-3.328380922
7207	PIK3CA H1047R	-3.785937307		7002	WT	-3.782094319		6576	WT	-3.314523983
2902	PIK3CA H1047R	-3.752671044		4740	WT	-3.781536689		1674	WT	-3.306363582
1341	PIK3CA H1047R	-3.713200593		4043	WT	-3.768330861		4980	WT	-3.298910641
3137	PIK3CA H1047R	-3.671303162		1752	WT	-3.766335		1249	WT	-3.295390818
858	PIK3CA H1047R	-3.656098973		1327	WT	-3.75265474		2719	WT	-3.263977737
4400	PIK3CA H1047R	-3.648945565		7195	WT	-3.751511698		7268	WT	-3.255103971
1183	PIK3CA H1047R	-3.647630834		1342	WT	-3.749278825		7707	WT	-3.23533579
3133	PIK3CA H1047R	-3.637861527		4078	WT	-3.742585256		1680	WT	-3.22963483
2886	PIK3CA H1047R	-3.635683444		3131	WT	-3.72416371		1162	WT	-3.228099405
3755	PIK3CA H1047R	-3.633896844		3229	WT	-3.722574233		1877	WT	-3.221786476
5407	PIK3CA H1047R	-3.620698893		660	WT	-3.69933605		3545	WT	-3.214370476
4977	PIK3CA H1047R	-3.594239755		3641	WT	-3.691392581		3773	WT	-3.211876318
1343	PIK3CA H1047R	-3.528465596		3797	WT	-3.68896346		3237	WT	-3.183472399
1191	PIK3CA H1047R	-3.528138963		7267	WT	-3.688019709		3912	WT	-3.175233205
7003	PIK3CA H1047R	-3.518689085		4101	WT	-3.685212057		1250	WT	-3.164742188
333	PIK3CA H1047R	-3.505950494		4376	WT	-3.68389676		4536	WT	-3.153060859
3649	PIK3CA H1047R	-3.482302675		1446	WT	-3.678458185		374	WT	-3.121493573
2500	PIK3CA H1047R	-3.474172366		3394	WT	-3.674039582		1440	WT	-3.06986259
1246	PIK3CA H1047R	-3.472941172		3351	WT	-3.661197578		4640	WT	-3.06892976
128	PIK3CA H1047R	-3.398987123		1238	WT	-3.651993793		5047	WT	-3.043657759
3928	PIK3CA H1047R	-3.389018818		1908	WT	-3.649164619		1030	WT	-3.041306836
4381	PIK3CA H1047R	-3.242833176		654	WT	-3.644300206		2738	WT	-3.028199647
2790	PIK3CA H1047R	-3.242606377		1332	WT	-3.62647911		2458	WT	-3.001607567
4894	PIK3CA H1047R	-3.198594833		2517	WT	-3.619144504		4453	WT	-2.977203662
1651	PIK3CA H1047R	-3.061275813		4421	WT	-3.615515568		3896	WT	-2.951557291
1460	PIK3CA H1047R	-3.052068185		2377	WT	-3.611342842		6315	WT	-2.930819908
189	PIK3CA H1047R	-2.979566525		4334	WT	-3.593236002		2208	WT	-2.900506837
4299	PIK3CA H1047R	-2.706043038		3083	WT	-3.590439793		1525	WT	-2.890165677
3731	PIK3CA H1047R/PIK3CA K111N	-3.41586907		2712	WT	-3.584821823		982	WT	-2.856414
1581	PIK3CA N345K	-3.711899822		4042	WT	-3.582789469		1523	WT	-2.83460463
7074	WT	-6.222115769		1646	WT	-3.573476775		3230	WT	-2.615669291
4425	WT	-4.283108827		4336	WT	-3.569554421		2773	WT	-2.592506423
3910	WT	-4.236606274		844	WT	-3.557154171		3904	WT	-2.535661361
4256	WT	-4.227384884		4444	WT	-3.545620421		4209	WT	-2.513167158
3399	WT	-4.203168905		1251	WT	-3.537184942		1302	WT	-2.164405169
2600	WT	-4.184640706		2605	WT	-3.534614829		2948	WT	-1.791293994
4188	WT	-4.160972808		265	WT	-3.521064939				

Supplementary Table 3. Reverse-Phase Protein Array (RPPA) analysis of c-MYC protein levels for a cohort of breast tumor samples with annotated *PIK3CA* mutation status.

Supplementary Methods

Luciferase activity assay. Snap-frozen mammary tissues were homogenized in 1X Reporter Lysis buffer (Promega). The lysates were cleared by centrifugation and analyzed using the Luciferase Assay System (Promega) on a Lumat LB 9507, following the manufacturer's instructions. We performed assays in triplicate and normalized relative light units to total protein levels.

Whole mounts, histology. The 4th mammary glands were mounted on glass slides, fixed overnight in glacial acetic acid/ethanol solution and transferred to 70% ethanol. The mounted slides were then rinsed in water and stained in a filtered solution of carmine/aluminum potassium sulfate. Glands were then dehydrated sequentially through 70%, 95%, and 100% ethanol for 20 min each, then defatted in toluene and stored in methyl salicylate.

Reverse transcription polymerase chain reaction (RT-PCR). Total RNAs from mammary tumors or normal mammary tissues were isolated using an Allprep DNA/RNA Mini Kit (Qiagen) and used to synthesize cDNAs with a High Capacity RNA-to-cDNA kit (Applied Biosystems). Quantitative PCR was performed with Taqman gene expression assays (Applied Biosystems). Human *PIK3CA*^{H1047R} and mouse *c-Myc*, *Pik3ca*, *c-Met*, *Mdm2* and *Gapdh* (as an endogenous control) were amplified with commercially designed Taqman gene expression assays (Applied Biosystems) and the Taqman gene expression master mix (Applied Biosystems). Quantitative expression data were acquired and analyzed with a 7300 Real-time PCR System (Applied Biosystems).

DNA copy number analysis. The relative copy number for *Myc* was determined by quantitative real time PCR using TaqMan Copy Number Assays (Applied Biosystems) and normalized to mouse endogenous reference gene *Tfrc* (Applied Biosystems, TaqMan Copy Number Reference Assay). All samples were analyzed in triplicate. Quantitative expression data were acquired and analyzed with a 7300 Real-time PCR System (Applied Biosystems).

Description of human breast cancer datasets

Cizkova M et al. (REF.18)

Expression levels of 43 ER-positive breast tumors from postmenopausal women at Rene Huguenin Hospital (Saint-Cloud, France) were profiled using Affymetrix microarrays. *PIK3CA* mutations of these tumors were detected by sequencing of RT-PCR products amplified from exons 9 and 20 and their flanking exons.

Kan et al. (REF. 19)

145 breast tumors and matched normal samples obtained from multiple commercial vendors were scanned for *PIK3CA* mutations using *Escherichia coli*-based mismatch repair detection. DNA copy number was assessed in 145 breast tumor samples using the Agilent 244K CGH array. Expression profile analysis was performed on RNA derived from 76 breast tumors using the Affymetrix Exon 1.0ST array.

Haverty PM et al. (REF. 20)

51 breast tumor samples in this cohort were profiled for copy number alterations with the Affymetrix 500K SNP array. These tumors were sequenced for mutations in selected genes commonly mutated in breast cancer including *PIK3CA*. The expression levels of these tumors and 22 normal breast samples were profiled using Affymetrix U113A and B microarrays.

Saal, et al. (REF. 21)

104 breast cancer tumor samples in this cohort were sequenced for *PIK3CA* mutations and analyzed on 2-color cDNA microarrays using the Stratagene Universal Human Reference RNA as the common reference sample.

Stemle-Hale et al (REF. 22)

There are 179 breast cancer samples in this cohort have *PIK3CA* mutation data. The *PIK3CA* mutations of these tumors were detected using Sequenom MassArray that detects activating mutations using primer extension. The c-MYC protein levels for these 179 breast tumor samples were quantified using Reverse-Phase Protein Array (RPPA) technology (REF. 23).